



Tracking millennial-scale climate variability during the last glacial period using aquatic productivity indicators from Lake Suigetsu, Japan

Vanessa Nowinski ^{a,*}, Alexander Francke ^a, John Tibby ^b, Takeshi Nakagawa ^c, Tony Hall ^d, Ikuko Kitaba ^c, Jonathan Tyler ^a, Suigetsu 2012 project members

^a Discipline of Earth Science, School of Physics, Chemistry and Earth Science, The University of Adelaide, SA 5005, Australia

^b Department of Geography, Environment and Population, The University of Adelaide, SA 5005, Australia

^c Research Centre for Palaeoclimatology, Ritsumeikan University, Shiga, 525-8577, Japan

^d Mawson Analytical Spectrometry Services, The University of Adelaide, SA 5005, Australia

ARTICLE INFO

Handling Editor: Dr P Rioual

Keywords:

Palaeoclimate
East Asian monsoon
Total organic carbon
Biogenic silica
Siderite
Fourier transform infrared spectroscopy

ABSTRACT

The East Asian monsoon, critical to nearly half the global population, faces an uncertain future amid rapid climate change. Palaeoclimate records reveal complex and shifting influences over East Asia that have varied across space and time during past episodes of abrupt climate change.

Untangling teleconnections that affect East Asian climate requires replicable, high resolution and precisely dated records, yet these are sparsely distributed worldwide. The varved sediments of Lake Suigetsu, Japan, are one such archive, offering significant potential to investigate millennial-scale variability in the East Asian monsoon. Here, we infer lake primary productivity as a tracer of regional climate during the last glacial period from 55 to 20 cal ka BP using sedimentary total organic carbon, biogenic silica and siderite, measured using Fourier transform infrared (FTIR) analyses. Lake productivity exhibits distinct millennial-scale events that align with palaeoclimate inferred from other lakes and speleothems in central Japan which, in turn, indicate a coherent picture of regional-scale hydroclimate variability. The Lake Suigetsu data varies with respect to synchronicity to Greenland ice core records, challenging the assumed spatial and temporal dominance of the North Atlantic and westerly winds on the East Asian monsoon, and supporting an alternative hypothesis of periodic dominance from the Southern Hemisphere.

1. Introduction

The East Asian monsoon (EAM) is a complex climate system that significantly influences water resources in one of the world's most densely populated regions, encompassing China, Japan, and Korea. Despite extensive research, there is still considerable uncertainty about how precipitation patterns in East Asia will evolve over this century. Key questions include whether precipitation will increase or decrease, how extreme variability will become, and whether regional patterns will shift (Gao et al., 2012; He, 2023; Xu and Fan, 2022; You et al., 2022).

Global instrumental climate records, dating back to the 1880s CE, have improved our understanding of the EAM on annual to decadal timescales (Chen et al., 2000, 2019; Huang et al., 2012; Lawrimore et al., 2011; Wang et al., 2000). However, these records do not capture the full range of climate variability that occurred in the geological past. As a result, it remains unclear whether short-term trends observed over the

last century can be generalised to long-term dynamics on timescales of centuries to millennia. This uncertainty is particularly significant when considering the teleconnections between EAM variability and abrupt climate changes linked to melting ice sheets and ocean circulation changes, both of which are projected by 2100 CE (Ditlevsen and Ditlevsen, 2023; Li et al., 2023; Naughten et al., 2023).

Greenland ice cores from the last glacial period reveal abrupt climate change events known as Dansgaard-Oeschger (DO) events, marked by episodes of rapid warming "Greenland Interstadials" followed by gradual cooling "Greenland Stadials" (Dansgaard et al., 1982). These oscillations are linked to changes in the Atlantic Meridional Overturning Circulation (AMOC), which regulates heat transfer between hemispheres (Broecker, 2010; Menzel et al., 2014; Oeschger et al., 1984). Similar climate fluctuations, such as Heinrich events and Antarctic Isotope Maxima, suggest a chain of interconnected climate changes during the last glacial period (Heinrich, 1988; Petit et al., 1999).

* Corresponding author.

E-mail address: vanessa.nowinski@adelaide.edu.au (V. Nowinski).

Synchronisation of Greenland and Antarctic ice cores via methane concentrations reveals an anti-phased relationship between temperatures in the Northern and Southern Hemispheres, supporting the “bi-polar see-saw” mechanism of interhemispheric thermal redistribution (Blunier et al., 1998; Broecker, 1998). These records provide important insights into the spatial drivers of climate variability and global climate teleconnections.

Studies of East Asian climate variability have linked changes in monsoon intensity to abrupt, millennial-scale climate events, specifically Dansgaard-Oeschger events. This link is thought to result from a teleconnection between the North Atlantic and East Asia, mediated by the influence of the westerly winds (Porter and An, 1995; Schulz et al., 1998; Tada et al., 1999). This connection has been further supported by high-resolution speleothem oxygen isotope records from China (An et al., 2000; Corriveau et al., 2020; Liang et al., 2019; Lu et al., 2022; Wang et al., 2001). However, other research challenges this mechanism, suggesting that additional factors drive variability of the East Asian monsoon (Barker and Knorr, 2007; Cai et al., 2006; Leuschner and Sirocko, 2000). Cai et al. (2006) was one of the first studies to propose an EAM-Antarctica teleconnection, a hypothesis supported by later research suggesting that processes in both the Northern and Southern Hemispheres influence monsoon intensity (Barker and Knorr, 2007; Beck et al., 2018; Cheng et al., 2020; Liang et al., 2022; Rohling et al., 2009; Shen et al., 2010). These conflicting findings highlight the uncertainties surrounding EAM variability and furthermore, the challenges posed by factors such as the type of climate archive used, geographical location, and proxy type. A key challenge remains geochronological precision, highlighting the rarity of well-dated records.

Lake Suigetsu, Japan, represents one of the world's most valuable terrestrial palaeo-environmental archives, with annual sediment laminations (varves) covering at least 50,000 years (Nakagawa et al., 2021). Radiocarbon dating of over 800 plant macrofossils, combined with tephrostratigraphy (Albert et al., 2024; McLean et al., 2018; Smith et al., 2013) and varve counting (Marshall et al., 2012; Scholz et al., 2012), provides a precise chronology that extends the terrestrial component of the IntCal20 radiocarbon calibration curve beyond the 13,900 yr BP tree-ring limit (Bronk Ramsey et al., 2020; Reimer et al., 2020).

This chronology has supported extensive palaeoenvironmental research, including pollen analysis (Nakagawa et al., 2021), diatom assemblage analysis (Kossler et al., 2011; Saito-Kato et al., 2013), luminescence profiling (Rex et al., 2022; Staff et al., 2024), and sedimentology (Fukusawa et al., 2002; Katsuta et al., 2007; Marshall et al., 2012; Suzuki et al., 2021). For research focusing on the timing of climate changes, it is crucial not only to have well-dated sediments, but also to use proxies that respond rapidly to those changes. Therefore, additional proxies sensitive to climate change are essential for improving understanding of the relationship between local and global climate systems.

This study investigates millennial-scale variability in sedimentary total organic carbon (TOC), biogenic silica (BSi) and siderite from Lake Suigetsu, as inferred by Fourier transform infrared spectroscopy (FTIR); a rapid and non-destructive technique for sediment compositional analysis. Previous work supports the interpretation that these data – particularly TOC, supported by organic matter C/N ratios and stable isotope ratios of carbon and nitrogen (Tyler et al., 2010) – reflect limnological processes, notably lake primary productivity, and offer indirect evidence of changing climate consistent with other regional records. The high precision chronology of Lake Suigetsu's sedimentary sequence coupled with the climatic influences from both the East Asian summer monsoon (EASM) and East Asian winter monsoon (EAWM), offer the opportunity to investigate the abrupt environmental and climatic fluctuations which occurred during the last glacial period in East Asia.

2. Regional setting

Lake Suigetsu is part of the ‘Mikata Five Lakes’: a system of

tectonically formed lakes located near the coast of the Sea of Japan in Fukui Prefecture, Honshu Island, Japan ($35^{\circ} 35' N$, $135^{\circ} 53' E$). At present, Lake Suigetsu has a maximum depth of 34 m, an area of 4.3 km^2 and a permanent chemocline at 3–8 m water depth following the construction of a canal connecting Lake Kugushi and Lake Suigetsu in 1664 CE which inundated the hypolimnion with seawater (Masuzawa and Kitano, 1982). Prior to this, Lake Suigetsu was a freshwater lake, with diatom species analysis indicating freshwater conditions from MIS 5d until the Holocene (Nakagawa et al., 2021). The lake is fed by outflow from Lake Mikata, which in turn is fed by the Hasu River. Regional climate data from the Tsuruga weather station located 16.5 km north-east of Lake Suigetsu, indicate an average annual air temperature of 14.7°C and annual precipitation of 2347 mm between 1898 and 2024 CE, and average annual snowfall of 186 cm recorded from 1953 to 2024 CE (Japanese Meteorological Agency, 2025). This climate pattern is largely influenced by monsoonal south-easterly winds from the Pacific Ocean, resulting in wet summers, and north-westerly winds crossing the Sea of Japan during winter, resulting in heavy snowfall, as supported by modern Lake Suigetsu water isotope data (Rex et al., 2024). This seasonal climate and hydrological setting, as well as the topography and bathymetry of Lake Suigetsu, is conducive to undisturbed and anoxic bottom waters, leading to the preservation and accumulation of seasonally characterised laminations, i.e. varves. The geology of the surrounding catchment of Lake Suigetsu is largely composed of greenstone (basalt, dolerite and volcaniclastic rock), sandstone and chert (Geological Survey of Japan, 2002).

3. Materials and methods

3.1. Coring and chronology

Sediment core ‘SG12’ was retrieved from the centre of Lake Suigetsu ($35^{\circ}35'07.93'' N$, $135^{\circ}52'56.40'' E$) during a deep drilling campaign in 2012 (SG12 Project Members). Drilling was operated by Seibu-Shisui Ltd. using a hydro pressure thin-walled piston sampler installed on a floating platform. Reaching a maximum sediment depth of 41.9 m, 139 m of core was collected from four drill holes (Suzuki et al., 2021).

As outlined in Section 1, the Lake Suigetsu sediment record is a key component of the IntCal Radiocarbon calibration dataset (Reimer et al., 2013, 2020). Chronological frameworks for these sediments have been developed and refined through varve counting, radiocarbon dating, and tephrochronology, with major contributions from coring campaigns including SG93, SG06, SG12, and SG14 (Bronk Ramsey et al., 2012, 2020; Francke et al., 2025; Marshall et al., 2012; Nakagawa et al., 2012; Scholz et al., 2012, 2018; Smith et al., 2013; Staff et al., 2013).

The presence of distinctive and regular event layers across all cores has enabled precise stratigraphic alignment over the last 70,000 years between cores SG93, SG06, SG12, and SG14. This alignment also allows the transfer of chronological frameworks between all cores. In this study, samples from the SG12 core were stratigraphically aligned with the composite Lake Suigetsu sequence (e.g. Staff et al., 2024; Suzuki et al., 2021) using the SG12 Correlation Model (Trinity - version Apr. 03, 2020) and age-depth model (version Sep. 25, 2020) (Figs. S1 and S2). The precise position of all the samples relative to marker layers with defined depth (“Holy Trinity”) are provided in the Supplementary Data.

Consistent with all SG projects, the LevelFinder software (version 7.7.4) was used to secure coherent depth/age control. All age estimates are reported in IntCal20 years BP (see Supplementary Data) and indicate that ages have been calibrated using the IntCal20 radiocarbon calibration curve and are equivalent to calibrated years before present (cal a BP), representing calendar years relative to 1950.

3.2. Sub-sampling

1.2 cm-wide LL-channels from the SG12 cores spanning 56,128 to 20,072 cal a BP were sub-sampled into 2249 1 cm-thick slices including

event layers < 3 mm. Event layers > 3 mm were removed prior to age-depth modelling and hence also removed from the composite record while sampling. To avoid seasonal bias due to changes in the sedimentation rate, samples were mechanically sliced at a 60° angle using a “Centi-slicer” which enables precise and consistent sub-sampling, as outlined in Nakagawa et al. (2021). Samples ($n = 398$) were selected at ~100-year intervals for further analyses.

3.3. Conventional TOC analysis

Conventional TOC analyses were conducted on 112 Suigetsu sediment samples to calibrate statistical models (Section 3.5.1) used for determining TOC content from FTIR spectra.

Samples were freeze dried, ground with an agate mortar and pestle, and acidified using 10 % HCl for 72 h. The samples were then rinsed with DI water from a Milli-Q system and centrifuged 3 times, redried, and accurately weighed into tin capsules using a Sartorius Cubis II d.p. balance. Samples were analysed by elemental analysis (EA) using a PerkinElmer 2400 series II CHNS/O Elemental Analyzer in CHN configuration. The combustion tube was packed using PerkinElmer EA-1000 Silver Vanadate & Silver Tungstate/Magnesium Oxide and the reduction tube was packed with PerkinElmer ‘Hi-Purity’ copper. The combustion temperature was 925 °C and reduction temperature was 640 °C. 4 mg of sample ($\pm 10\%$) were analysed with results calibrated to 4 mg of Perking Elmer Organic Analytical Standard of Acetanilide with known abundances of carbon (71.09 %), hydrogen (6.71 %) and nitrogen (10.37 %). The accepted error range between standards from the instrument validation was $\pm 0.3\%$ for carbon, hydrogen and nitrogen calculated against 12 replicates. TOC analyses were conducted in the University of Adelaide’s Mawson Analytical Spectrometry Services facility.

3.4. Fourier transform infrared spectroscopy (FTIR)

FTIR is a high throughput and non-destructive method for inferring sediment composition. The 398 selected sub-samples were freeze dried and ground with an agate mortar and pestle and kept in an air-conditioned laboratory environment prior to analyses for at least 24 h. Undiluted (no KBr added) samples (~0.01–0.1 g) were scanned 50 times over a wavelength range of 400–3750 cm⁻¹ (reciprocal centimetres) at 1 cm⁻¹ resolution using a Shimadzu IRSpirit FTIR spectrophotometer with deuterated L-alanine doped triglycine sulphate (DLATGS) detector, hosted in the Adelaide Spectroscopy facility at the University of Adelaide. Analysis was performed using ATR (attenuated total reflectance). Linear baseline correction and normalisation was applied to all FTIR spectra prior to further data processing. Normalisation was performed using MATLAB’s msnorm function, which standardises the area under the curve (AUC) of each spectrum to the group median. Specifically, $y_{Out} = \text{msnorm}(X, \text{Intensities})$ returns the normalised data, while $[y_{Out}, \text{normParams}] = \text{msnorm}(X, \text{Intensities})$ also provides the normalisation parameters (normParams) used in the process. Baseline correction performs a linear correction of the spectra so that two points (3750 and 2210–2200 cm⁻¹) equals zero to obtain a consistent baseline for all spectra. Combined with normalisation, which accounts for variations in total transmittance due to slightly different sample amounts, baseline correction accounts assure independence of measurement conditions. Baseline correction and normalisation was computed using MATLAB (R2022a).

3.5. Statistical analyses

3.5.1. Total organic carbon (TOC)

Pearson et al. (2014) previously developed a Lake Suigetsu-specific training set to infer sediment TOC from Fourier transform near infrared reflectance spectroscopy (FT-NIRS) from the lake’s sediments using partial least squares regression (PLSR) models. Here, we develop a

new bootstrap (1000 iterations) PLSR model to infer TOC for the samples analysed in this study by means of calibrating baseline corrected and normalised FTIR spectra against conventional elemental analyses for organic carbon, following the approach of Rosén et al. (2010, 2011) and Pearson et al. (2014). Developing a new Suigetsu PLSR is necessary since Pearson et al. (2014) used FT-NIRS. Coefficients estimates of 1000 bootstrap PLSR models were averaged to quantify TOC contents. Reference TOC data (EA analyses) and all FTIR spectra were z-score standardised (mean = 0, standard deviation = 1) prior to PLSR modelling to obtain consistent results during bootstrapping. Data processing and statistical analyses of FTIR spectra was performed in MATLAB R2022a. Validation of FTIR-inferred TOC was made through comparison with previously published data (Francke et al., 2025).

3.5.2. Siderite

Relative abundance of siderite in the Lake Suigetsu sediments was inferred by integrating the diagnostic bending vibrations for siderite (854–867 cm⁻¹) peak areas, which are representative for the relative mineral abundance (Fig. S3) (Chukanov, 2013; White, 1974). This approach was previously applied for lacustrine sediments by Lacey et al. (2016). Data processing and statistical analyses of FTIR spectra was performed in MATLAB R2022a.

3.5.3. Biogenic silica (BSi)

BSi levels were calculated using an end-member mixing model, following Swann and Patwardhan (2011). FTIR spectra for two end members were characterised: (a) a pure, synthetic biogenic silica standard (NFC), (b) averaged FTIR spectra from eight Lake Suigetsu sediment samples from the studied interval, dissolved in 1M sodium hydroxide 2 times, for 30 min at 80 °C. Microscopic analyses were performed to ensure the absence of diatoms after treatment. The FTIR spectra of these endmembers conformed to typical spectra for pure BSi, and an amalgamation of organic matter, silts and clays, respectively (FTIR spectra for BSi and BSi-free endmembers displayed in Fig. S4). A ‘mass-balance’ matrix T containing 10,000 reference spectra representing 0.01 % change in BSi for each reference spectra (Fig. S4) was developed for wavelengths between 700 and 1300 cm⁻¹ between these two endmembers. Subsequently, BSi concentration were estimated by fitting each individual sample FTIR to the mass balance matrix. The high number of reference spectra is required to reduce the *residue c* (% of normalised FTIR spectra) between the sample FTIR spectra and T . Best model fit was determined by detecting lowest *residue c* value for each fit. Data processing and statistical analyses of FTIR spectra was performed in MATLAB R2022a.

3.6. Determining diatom dissolution

To assess the extent of diatom dissolution in the lake sediments and its potential impact on BSi concentrations, 16 samples from approximately 40–35 cal ka BP were prepared for microscopic analysis. This interval was selected because it encompasses a period of high variability in TOC, BSi and siderite levels, and thus represents a range of chemical environments that may influence diatom preservation. Sample preparation followed standard protocols as outlined in Battarbee et al. (2001).

4. Results

4.1. Statistical performance of the TOC model

Of the 112 conventional TOC values, four samples were excluded from the calibration dataset due to irregular FTIR spectra (see Fig. S5). Additionally, two samples with irregular spectra were removed from the dataset of unknowns, resulting in a final sample size of $n = 396$ for TOC, BSi, and siderite estimates.

The optimal TOC partial least squares regression (PLSR) model included 14 components, achieving a cross-validated R^2 value of 0.97

and a root mean squared error (RMSE) of 0.2 %. The 14-component model was identified as optimal based on the relationship between cross-validated RMSE and the number of model components, selecting the model with the lowest cross-validated RMSE prior to the inflection towards a plateau (see Fig. S6). Modelled TOC were further validated by comparison with independently measured TOC from a separate sediment core collected in 2006 (Francke et al., 2025). Although minor discrepancies exist between the two datasets due to differing composite depth intervals (see Supplementary Data), the 14-component model effectively reproduces the main structure and range of variability of the independent record.

Further model component reduction – guided by the principle of parsimony – resulted in models that failed to reproduce the full range of TOC values, based on the independent test dataset. Specifically, successive removal of components led to a progressive underestimation of minimum and maximum TOC values, deviating further from the independently measured extremes (0.57–7.01 %). Given that the 14-component model already slightly underestimates those extremes (0.29–6.63 %), it was deemed the most parsimonious configuration that preserved alignment with the validation data. Additional model performance metrics and validation plots are provided in the Supplementary Data and are shown in Fig. S6.

4.2. Statistical performance of the BSi model

The BSi model is based on an endmember approach and does not rely on a conventional calibration dataset, therefore model performance was assessed using the *residue c* values for each sample. The lowest residue values for the best-fit range from 1.5 % to 11.9 % (median = 5.7 %), similar to the best model output reported by Swann and Patwardhan (2011). These low residue values indicate a good overall fit between observed and modelled spectra. Residue values for all individual samples are provided in the Supplementary Data.

4.3. Temporal variability in FTIR-inferred TOC, BSi, and siderite

Sediments deposited between circa 56,100 to 20,100 cal a BP (IntCal20) in Lake Suigetsu exhibit distinct fluctuations in FTIR-inferred total organic carbon (TOC), biogenic silica (BSi), and siderite content (Fig. 2). From 55 to 37 cal ka BP during MIS 3, TOC and BSi levels are generally low (up to 4.5 % and 24.6 %, respectively), with notable maxima at approximately 55 ka, 50 ka, and 47 cal ka BP. During this period, siderite levels remain persistently high (~0.2 peak area). From 37 to 20 cal ka BP, encompassing the MIS 3/2 boundary, TOC and BSi content are at their highest (up to 6.2 % and 43.8 %, respectively), with notable maxima at approximately 36 ka, 34.5 ka, and 32 cal ka BP, before decreasing after 30 cal ka BP. Siderite levels are generally lower (~0.1 peak area) in this interval, with the exception of a prominent spike (~0.5 peak area) at 30.5 cal ka BP, which coincides with a minima in TOC and BSi.

TOC and BSi levels have a positive correlation ($R^2 = 0.41$, i.e. Pearson's R of approx. 0.64) between 55 and 20 cal ka BP, with the exception of two periods at 40 and 52 cal ka BP that exhibit no correlation (Fig. 3). In the sediments deposited during these periods, the correlation between siderite and BSi, and siderite and TOC, respectively, slightly increase (Fig. 3). Apart from these periods, TOC and BSi concentrations display varying correlation to siderite levels.

5. Discussion

5.1. Framework for interpreting TOC, BSi and siderite content in the sediments of Lake Suigetsu

Reconstructing past environments and climates from sediment composition data requires careful consideration of the environmental mechanisms which drive sediment deposition. To address this, we first

establish a foundation for interpreting variations in total organic carbon (TOC), biogenic silica (BSi), and siderite levels at Lake Suigetsu by comparing our new data with previous research from Lake Suigetsu. We conclude that changes in TOC and BSi reflect variations in aquatic primary productivity, while changes in siderite content indicate episodes of deep vertical circulation within the lake; both of which are driven by changes in climate.

5.1.1. Total organic carbon (TOC)

The organic carbon content of lake sediments reflects a composite of molecular types from various organisms, such as higher plants, animals and microorganisms, sourced from lakes and their surrounding catchments (Cohen, 2003). Changes in total organic carbon (TOC) in lake sediments therefore reflect a combination of processes that influence the production, transport and preservation of organic carbon, all of which can be affected by direct and indirect factors such as nutrient availability, temperature, and variation in rainfall (Meyers and Ishiwatari, 1993).

In lake sediments of primarily aquatic sourced organic carbon, TOC has been interpreted as a tracer for climate-driven lake productivity (Kigoshi et al., 2014; Kudo and Kumon, 2012; Leng et al., 2013; Meyers and Ishiwatari, 1993). However, this climate signal can be affected by the input of terrestrial organic material from the catchment, particularly during extreme events such as earthquakes or flooding, which can lead to significant deposition of terrestrial matter. To distinguish the primary source of TOC, the sedimentary carbon-to-nitrogen (C/N) ratio can be used to determine if the organic matter is largely derived from terrestrial plant material, as indicated by a high C/N ratio. For Lake Suigetsu where organic material is primarily deposited during the summer (Schlolaut et al., 2012), C/N ratios for the time period of present day - 140 ka exhibit low values, implying primarily aquatic sourced organic carbon (Francke et al., 2025). Previous studies spanning the period from 21 to 6 cal ka BP also suggest that the majority of organic matter is derived from aquatic sources, as indicated by $\delta^{13}\text{C}$ and $\delta^{15}\text{N}$ isotopic analysis of chlorins (Tyler et al., 2010). It is likely that most incoming terrestrial particulate matter from the Hasu River is filtered out by Lake Mikata before reaching Lake Suigetsu (Fig. 1). These lines of evidence suggest that Lake Suigetsu TOC reflects internal lake productivity rather than terrestrial input.

TOC concentration in lake sediments can also be affected by preservation. Poor organic carbon preservation in lake sediments has been suggested to undermine the interpretation of TOC as a proxy for primary productivity (Lehmann et al., 2002; Sobek et al., 2009). However, in Lake Suigetsu TOC is well preserved as indicated by the preservation of highly labile chlorophyll pigments (Tyler et al., 2010) and the presence of varves, which indicate constant anoxia and the absence of bioturbation (Anderson and Dean, 1988; Kelts and Hsii, 1978). We therefore interpret fluctuations in TOC at Lake Suigetsu to reflect changes in aquatic productivity through time.

5.1.2. Biogenic silica (BSi)

The biogenic silica (BSi) content of lake sediments reflects silica derived from aquatic biological sources - particularly diatoms, but also chrysophytes and sponges as well as phytoliths from terrestrial and aquatic higher plants (Cohen, 2003; Conley and Schelske, 2001). Factors that affect the productivity of silicic aquatic organisms include nutrient availability, pH, turbidity, water temperature, and duration of ice-free periods (Cohen, 2003; Conley and Schelske, 2001). As such, various studies have interpreted BSi to reflect regional hydrology and climate change (Douglas and Smol, 2010; Fortin and Gajewski, 2009; McKay et al., 2008; Schelske et al., 1987).

For the Lake Suigetsu sediments, we interpret BSi to primarily reflect diatom abundance and productivity. This is evidenced by the preservation of consistent diatom-rich varves which are suggested to form primarily in autumn and spring following lake overturn (Schlolaut et al., 2012). Additionally, there was no evidence of other significant sources

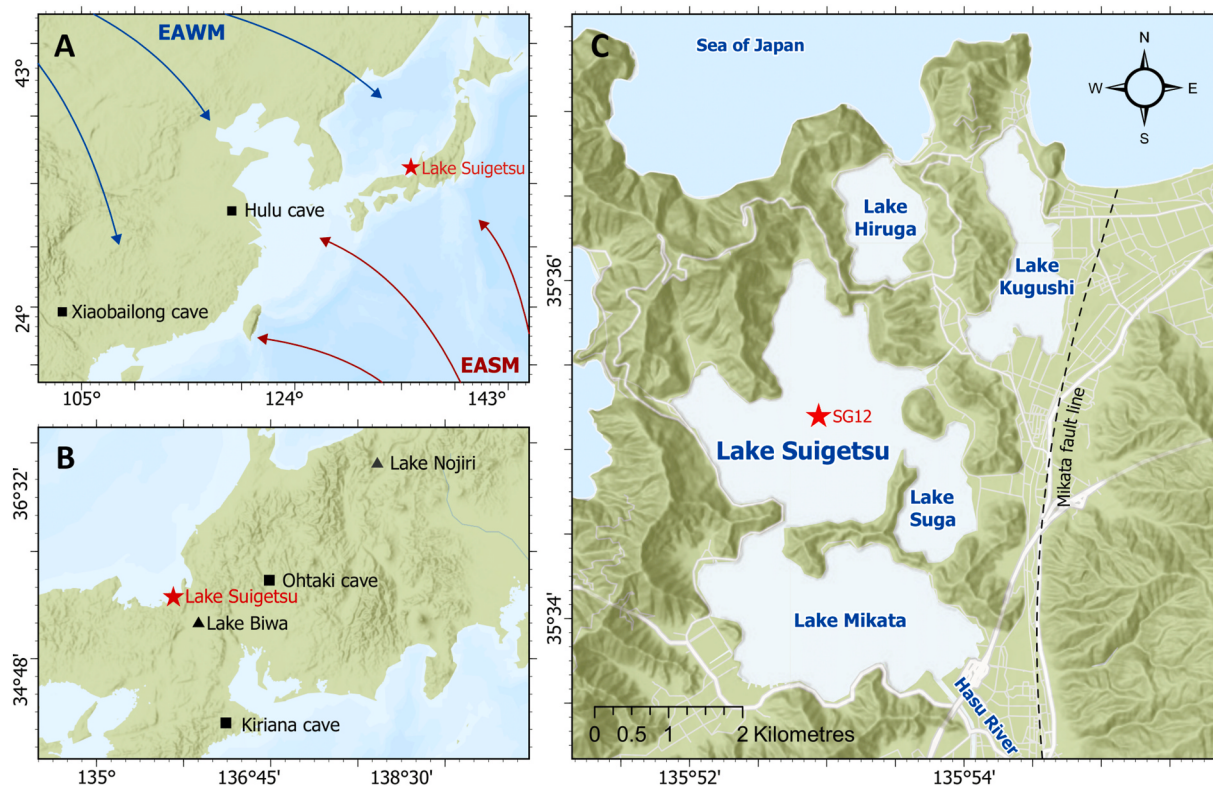


Fig. 1. Location of environmental records from Lake Suigetsu, central Japan and East Asia from the last glacial period. (A) Lake Suigetsu in relation to speleothem records obtained from Hulu and Xiaobailong caves in China. EAWM = East Asian winter monsoon, EASM = East Asian summer monsoon. (B) Lake Suigetsu in relation to key palaeoclimate records from central Japan. (C) Lake Suigetsu in relation to the 'Mikata Five Lakes'. Lake Suigetsu is primarily fed by Lake Mikata, which is fed by the Hasu River. Basemaps: Hillshade and World Terrain from Esri (scale of map A (1:19,000,000), map B (1:3,000,000), and map C (1:41,000)).

of biogenic silica, such as sponge spicules and phytoliths in the samples analysed by microscopy.

Dissolution of diatom frustules can potentially alter BSi concentrations and therefore complicate their use as a climate proxy (Barker, 1992; Battarbee et al., 2005; Flower, 1993). However, we expect high preservation of diatom frustules in Lake Suigetsu due to the abundance of well-preserved yet lightly silicified *Fragilariaeaceae* and *Cyclostephanos* species. Furthermore, the environmental conditions that typically promote accelerated diatom dissolution, such as high salinity, high water temperature and elevated pH (Kamatani, 1982; Lewin, 1961; Ryves et al., 2001), are uncommon in Lake Suigetsu. The presence of varves, which indicate constant anoxia and limited bioturbation, further support the preservation of diatom frustules (Bradbury et al., 2002; McMinn, 1995). As a result, elevated BSi concentrations in the Lake Suigetsu sediments likely reflect periods of increased diatom productivity, which is driven by higher nutrient availability and delivery, particularly promoted by warmer and wetter conditions (Colman et al., 1995; Conley and Schelske, 2001; Iwamoto and Inouchi, 2007; Prokopenko et al., 2001; Xiao et al., 1997).

The positive correlation between the Lake Suigetsu TOC and BSi records (Fig. 2) further indicates that they are both influenced by the same driver, aquatic primary productivity. The instances of decoupling of TOC and BSi concentrations (Fig. 3) could therefore be interpreted as increased terrestrial organic carbon input and, or decomposition of organic carbon or diatom frustules. However, consistently low TOC/TN values reported for this period (Francke et al., 2025) as well as the strong correlation for the majority of the record suggests that changes in productivity are largely driven by within-lake processes, and therefore can confidently be interpreted as a record for palaeo-productivity. We therefore interpret the fluctuations in both the BSi and TOC records from Lake Suigetsu as reflecting changes in aquatic productivity, likely linked to warmer and wetter conditions that promote biological productivity

and enhance nutrient mobilisation and delivery.

5.1.3. Siderite

Siderite, an iron carbonate mineral occasionally found in lake sediments, is suggested to form through several processes, including (1) precipitation from solution under anoxic conditions (Ozawa et al., 2017), (2) mineralisation in porewaters near the sediment-water interface (Giresse et al., 1991), and (3) during diagenesis within the sediment (Vuillemin et al., 2019). The formation of siderite requires low sulfide levels, high CO₂ partial pressure, and oxygen-reduced conditions (Bahrig, 1989; Curtis and Spears, 1968; Stumm and Morgan, 2012). As a result, the deposition of siderite has been used to understand lake processes such as anoxia, catchment weathering, methanogenesis, and lake turnover (Bahrig, 1988; Berner, 1971; Leng et al., 2013). While the processes determining siderite concentrations in lake sediments are less well understood than TOC and BSi, it is generally inferred that higher levels of siderite indicate periods of more effective lake water mixing (Bahrig, 1988; Ozawa et al., 2017; Vuillemin et al., 2023).

In the sediments of Lake Suigetsu, siderite appears as distinctive seasonal layers occurring predominantly in the autumn deposits (Marshall et al., 2012; Schlolaut et al., 2012). Since siderite is the most frequent and consistent seasonal layer in the Lake Suigetsu varve record, it has been suggested that the lake undergoes annual stratification during warmer seasons, followed by lake overturn during colder seasons (Marshall et al., 2012; Schlolaut et al., 2012). Lake overturn brings trapped particulate matter suspended in the water column that contains iron, to the anoxic lake bottom. Suggested mechanisms for lake overturn include the cooling of surface waters due to cooling air temperatures, influx of cold-water pulses from snowmelt, and increased physical mixing from wind, all of which disrupt the epilimnion formed under warmer conditions (Imboden and Wüest, 1995; Ye et al., 2019). These factors indicate that siderite formation is likely to increase as the climate

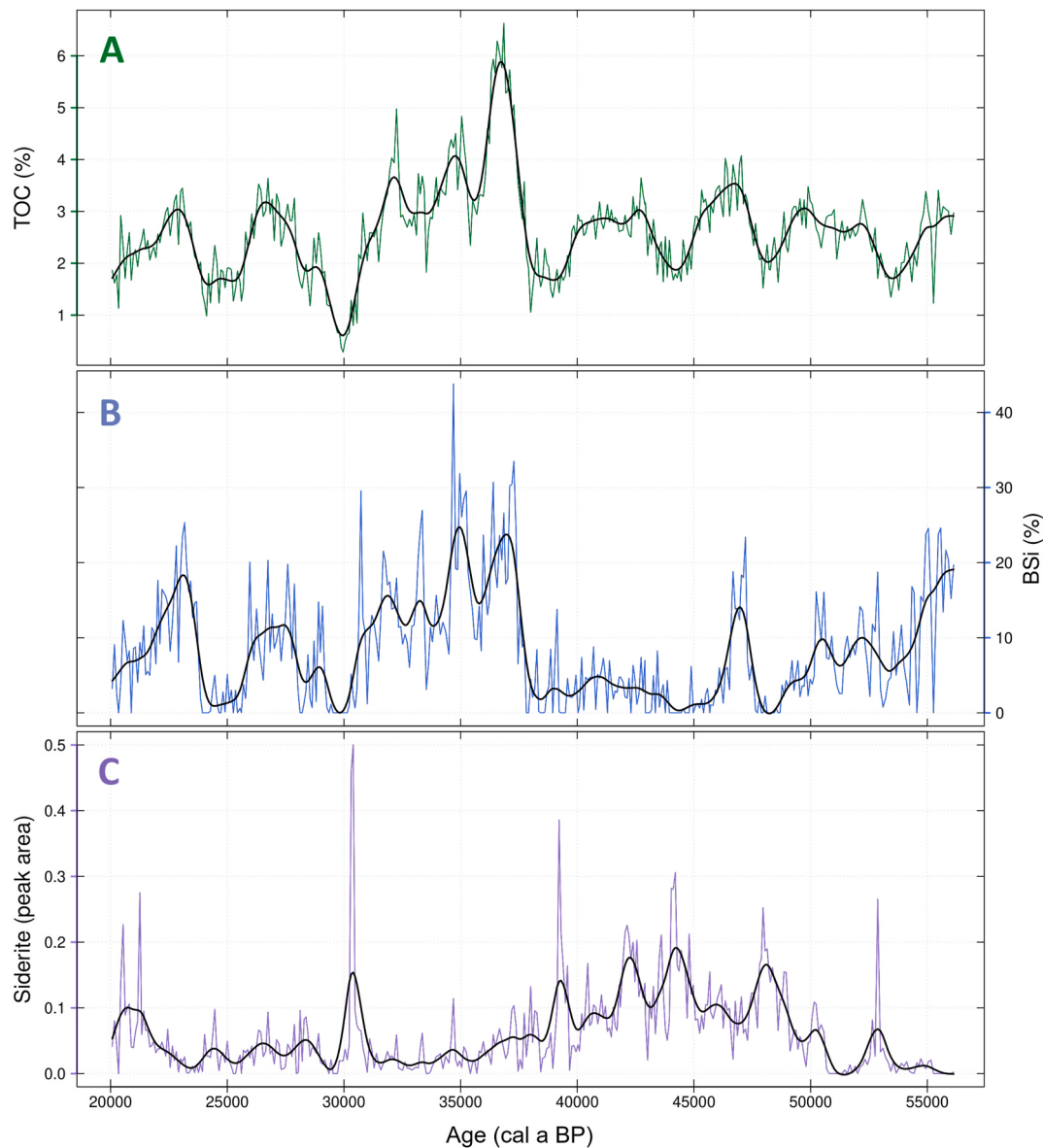


Fig. 2. Variations in Lake Suigetsu sediment composition over time using SG12 cores spanning 56,128 to 20,072 cal a BP (IntCal20) (age model: version Sep. 25, 2020 and correlation model: SG12 Correlation Model (Trinity) version Apr. 03, 2020). (A) Total organic carbon (TOC), (B) biogenic silica (BSi), and (C) siderite concentrations are inferred from Fourier transform infrared (FTIR) spectra. Datasets for TOC, BSi and siderite concentrations are overlaid with a spline curve with lambda = 0.0000009 (black).

transitions from a warm and wet, to a cool and more wind-stressed state. Although fluctuations in siderite relative to TOC and BSi could result from mutual dilution, we consider this is unlikely. The strong positive correlation between TOC and BSi, alongside the lack of correlation with siderite, suggests that the observed trends reflect distinct climate responses rather than mutual dilution effects. Therefore, we interpret increased siderite levels to reflect an increase in deep mixing events which are potentially driven by a shift to colder and more wind-stressed climate (Schlolauf et al., 2012).

5.1.4. Lake Suigetsu productivity proxies as indicators of monsoonal variability

At Lake Suigetsu, periods of higher lake productivity are inferred from changes in TOC and BSi, which we interpret as indicators of aquatic and diatom productivity, respectively. As previously discussed, periods of increased productivity are likely linked to warmer and wetter climate, which in turn drives enhanced nutrient mobilisation and delivery. Given that warmer and wetter climates in Japan are associated with an

enhanced East Asian summer monsoon (EASM), it is plausible that variations in TOC and BSi concentrations may reflect fluctuations in the intensity of the EASM.

Following this interpretation, cooler winter months in Japan, dominated by the East Asian winter monsoon (EAWM), may be linked to increases in siderite levels, which indicate reduced thermal stratification and increased mixing during transitions to a colder, wind-stressed climate. Therefore, increases in siderite levels may reflect a strengthening of the EAWM, causing cooler conditions, heightened winds, and increased snowfall at Lake Suigetsu—all of which are factors that could trigger lake overturn by disrupting the thermal stratification of the lake.

5.2. Regional and global coherence of climate inferred from Lake Suigetsu

5.2.1. Central Japan

Variability in TOC and BSi, interpreted as indicators of primary productivity in Lake Suigetsu, exhibit fluctuations similar to those observed in other last glacial period Japanese lake TOC records, namely

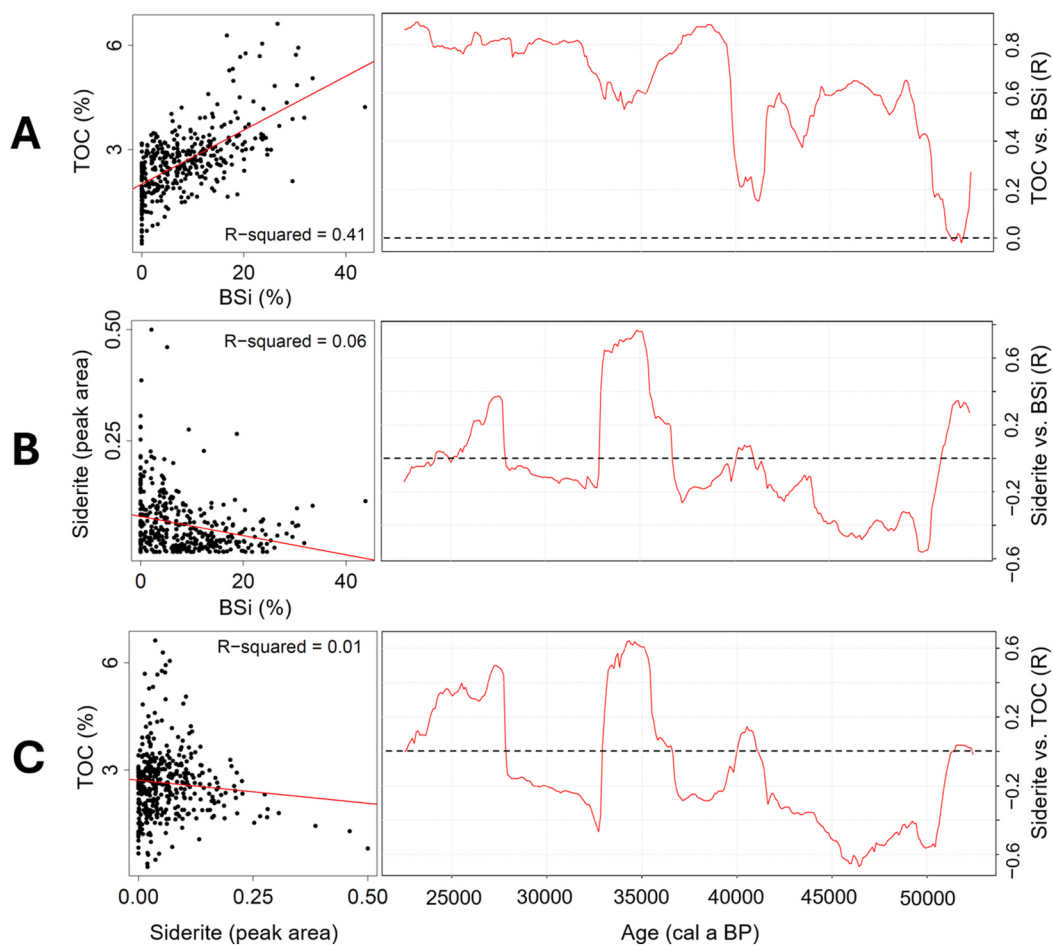


Fig. 3. Linear regression (R^2) and moving window correlation (Pearson's R) between (A) total organic carbon and biogenic silica (B) siderite and biogenic silica; and (C) siderite and total organic carbon. Analyses for the moving window correlation were conducted on 100-year interpolated and resampled datasets, with a 5000-year moving window.

those from Lakes Biwa and Nojiri (Fig. 4 and Fig. S7). At Lake Biwa, the TOC record is also considered a proxy for aquatic productivity, with C/N ratios indicating that organic matter largely derives from aquatic plankton (Kigoshi et al., 2014). As a result, the TOC record from Lake Biwa, supported by correlation with BSi content, has been interpreted as an indicator of aquatic primary productivity and as reflective of changes in precipitation and temperature; where increased TOC concentrations are associated with warmer and wetter climate (Iwamoto and Inouchi, 2007; Kigoshi et al., 2014; Meyers et al., 1993).

Similarly, Lake Nojiri, located approximately 225 km north-east of Lake Suigetsu and sharing a similar modern climate, with high precipitation during both summer and winter, also displays patterns of environmental change that closely resemble those from Lake Suigetsu (Kudo and Kumon, 2012; Kumon et al., 2003). Like Suigetsu and Biwa, the C/N ratios from Lake Nojiri indicate a predominance of aquatic-derived organic carbon (Kudo and Kumon, 2012), which has been interpreted as a proxy for temperature with increased TOC levels indicating warmer climate. The Nojiri TOC record also shows rapid centennial- to millennial-scale fluctuations, with many of the major maxima and minima events aligning with those recorded at Lakes Suigetsu and Biwa (e.g., maxima at 47 and 37 cal ka BP, and minima at 29 cal ka BP), however, this is limited by age uncertainties (Fig. 4 and Fig. S7). Regardless, the similarities among the TOC records from Suigetsu, Biwa and Nojiri provide important validation of the climate significance of our data and suggest that the TOC record from Lake Suigetsu reflects broader regional climate rather than local catchment dynamics.

In addition to Japanese lake TOC records, speleothem records from

Ohtaki Cave and Kiriana Cave in central Japan (Mori et al., 2018) exhibit fluctuations that also align with excursions observed at Lake Suigetsu. Periods of cooler and wind stressed climate, inferred from low primary productivity (indicated by low TOC and BSi) and increased lake mixing (indicated by high siderite) at Lake Suigetsu, align with cooler periods inferred from high $\delta^{18}\text{O}$ values from speleothem records collected from Ohtaki and Kiriana caves (Mori et al., 2018) (Fig. 4 and Fig. S7). These cool conditions occur in both the Lake Suigetsu and central Japan speleothem records at approximately 48 to 46 ka and 39 ka, and during 30 ka and 24 ka at Kiriana Cave and Lake Suigetsu, when Kiriana Cave exhibits consistently cool conditions. Additionally, periods of higher productivity at 50, 42, and 39 cal ka BP align with warmer intervals recorded in the Japanese speleothems. However, the coherence between warm intervals inferred from Japanese speleothem records and higher productivity from Lake Suigetsu records is not always consistent. For example, intervals of enhanced EASM activity observed at Lake Suigetsu during 26 and 23 cal ka BP are not evident in the Kiriana Cave speleothem record. This is possibly due to the archive type, as suggested by Mori et al. (2018), who observed that the speleothem records from Ohtaki and Kiriana caves were less sensitive to warm interstadial periods compared to lake TOC records from Japan, which appeared to show both stadial and interstadial excursions.

Nevertheless, the coherence in fluctuations recorded in speleothems in central Japan and the TOC and BSi records from Suigetsu, further support the interpretation of the lake sediment geochemical records as being reflective of regional climate variability linked to the East Asian monsoon during the last glacial period.

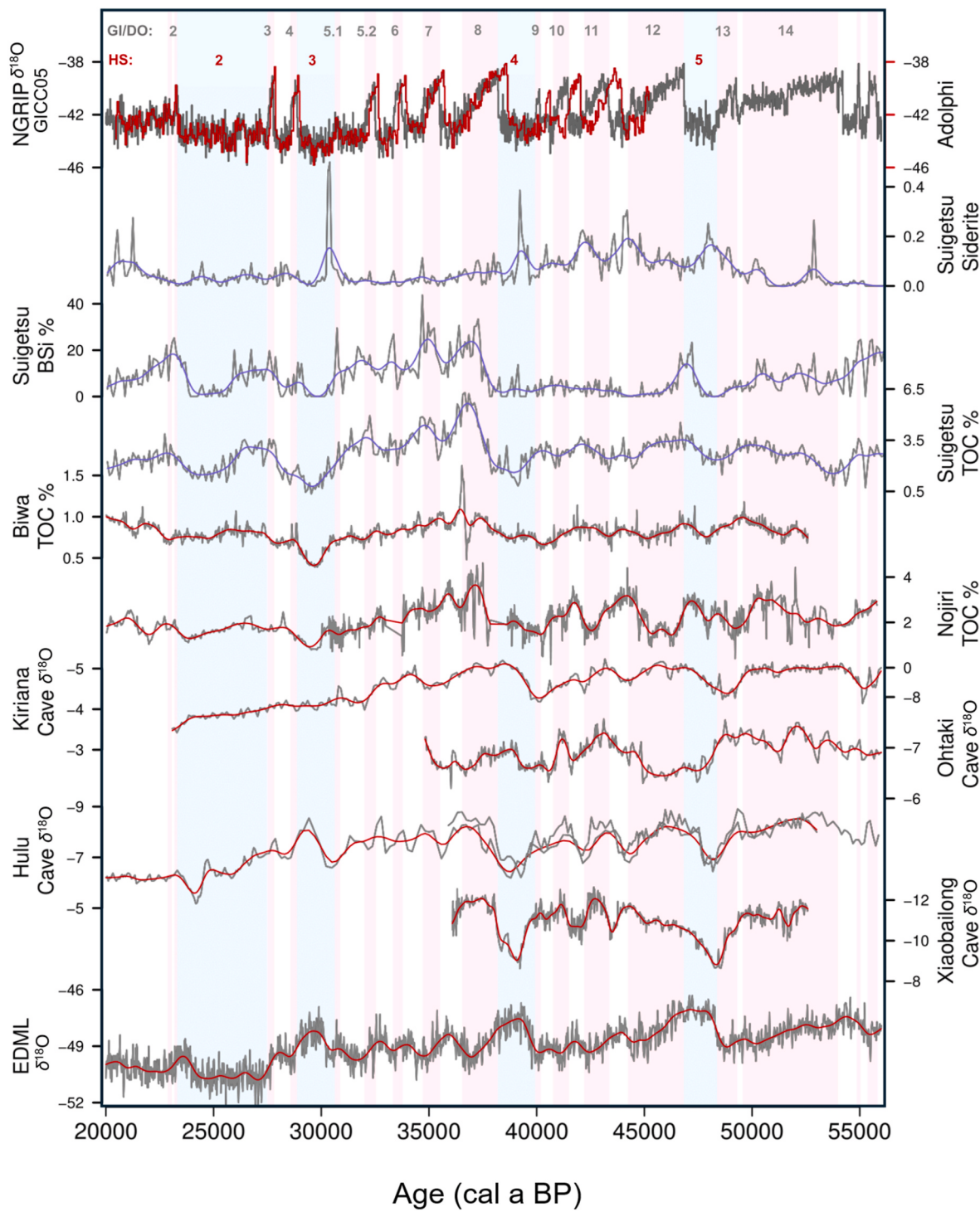


Fig. 4. Regional and global climate records compared to Lake Suigetsu TOC, BSi and siderite records. Comparison records include the North Greenland Ice Core Project (NGRIP) $\delta^{18}\text{O}$ with GICC05 (Rasmussen et al., 2014; Seierstad et al., 2014) (dark grey) and Adolphi et al. (2018) (dark red) chronologies, Lake Biwa sedimentary TOC (Kigoshi et al., 2014), Lake Nojiri sedimentary TOC (Kumon et al., 2003), Kiriana and Ohtaki Caves speleothem $\delta^{18}\text{O}$ (Mori et al., 2018), Hulu Cave $\delta^{18}\text{O}$ for speleothems MSD and MSL (Wang et al., 2001), Xiaobailong Cave speleothem $\delta^{18}\text{O}$ (Cai et al., 2006), and Antarctica EPICA Dronning Maud Land (EDML) $\delta^{18}\text{O}$ WD2014 (Buizert et al., 2015). Heinrich stadials (light blue bars numbered in red) and Greenland interstadials (light pink bars numbered in dark grey) follow age ranges as published in Rasmussen et al. (2014). Datasets are overlaid with a spline curve with lambda = 0.0000009 (blue for new datasets, red for comparison datasets).

5.2.2. East Asia

Speleothem records from various caves across China, including Hulu, Xiaobailong, Sanbao, and Dongge caves, have been instrumental in interpreting the variability of the East Asian monsoon and understanding regional climate patterns (Cai et al., 2006; Cheng et al., 2009;

Dykoski et al., 2005; Kelly et al., 2006; Liang et al., 2019; Wang et al., 2001, 2008; Yuan et al., 2004). Given the proximity of Lake Suigetsu to these sites, we hypothesised that the environmental changes inferred at Lake Suigetsu may reflect those observed in the Chinese speleothems.

Speleothem $\delta^{18}\text{O}$ data from Hulu cave, located 1570 km west of Lake

Suigetsu (Fig. 1), exhibit climate fluctuations that align, within age uncertainties, with those recorded in the Suigetsu TOC and BSi records (Fig. 4 and Fig. S7). Notably, periods interpreted to indicate a weakened summer monsoon show similar timing in both records, particularly at 48 ka (although limited by Hulu Cave age uncertainties; Fig. S7), and at 39, 30, and 24 ka, reflecting patterns observed in the aforementioned Japanese speleothems from Ohtaki and Kiriana caves (Section 5.2.1). Similarly, another speleothem record from Xiaobailong Cave, located 3350 km south-west of Lake Suigetsu (Fig. 1), also displays similar timing for periods of weakened EASM inferred from Lake Suigetsu at 48 and 39 ka (Cai et al., 2006), while similar excursions have also been reported in TOC levels from Lake Sihailongwan in north-east China (Mingram et al., 2018).

While periods of strengthened EASM exhibit less coherence between Hulu Cave and Lake Suigetsu, they still reveal comparable timing and shape of symmetric strengthening and weakening, particularly during 48, 37, 36 and 23 cal ka BP (Fig. 4 and Fig. S7). The reduced coherence during periods of enhanced EASM, such as at 43 and 42 cal ka BP, may be attributed to the location of Lake Suigetsu at the periphery of the EASM, potentially indicating that during some periods, the extent of the summer monsoon was restricted and only reached eastern China. Another possible mechanism for the observed climate variations between China and Japan is the shifting of the westerly jet in relation to the Tibetan Plateau (Chiang et al., 2015; Schiemann et al., 2009). This hypothesis has previously been suggested for the Lateglacial to Early Holocene transition (16–10 cal ka BP) at Lake Suigetsu by Nakagawa et al. (2021), and has also been inferred from Japan Sea sediments, which suggest rapid north-south shifts in the jet path during Dansgaard-Oeschger events (Nagashima et al., 2011). During warm interstadials, the northward migration of the ITCZ likely pushed the westerly jet north of the Tibetan Plateau, bringing a relatively dry climate to Lake Suigetsu compared to a wetter climate at Hulu Cave. In contrast, during cold stadial periods, when the jet shifted south of the Plateau, both Lake Suigetsu and Hulu Cave would have been affected by the same jet path, leading to more similar climate conditions at both sites. This mechanism may explain the inconsistent relationship between climate records from Japan and China during warm interstadial periods.

Nonetheless, the similarities in cold phases between the Lake Suigetsu, Hulu Cave and Xiaobailong Cave records provide compelling evidence for periodic climatic coherence during the last glacial period, suggesting that the sediments of Lake Suigetsu reflect climatic conditions not only in Japan, but across East Asia.

5.2.3. Greenland and Antarctica

The synchronisation of Greenland and Antarctic ice core records via methane concentrations enable us to investigate spatial drivers of climate systems in relation to the abrupt climate changes recorded in the Southern and Northern polar regions. Previous studies of East Asian climate records, including Hulu Cave, have inferred a potential teleconnection between the North Atlantic and the EAM region, via the westerly jet, as supported by correlations with Greenland ice cores (An et al., 2000; Cheng et al., 2009; Corrck et al., 2020; Liang et al., 2019; Lu et al., 2022; Porter & An, 1995; Schulz et al., 1998; Shen et al., 2010; Tada et al., 1999; Wang et al., 2001).

If the proposed teleconnection also influenced climate at Lake Suigetsu, we would expect the onset of warm interstadials recorded in the Greenland ice cores to occur *before* or during transitions to a warmer and wetter climate at Lake Suigetsu caused by strengthening of the EASM. While we observe alignment during Greenland interstadials (GI) 8 and 7, there are instances where warming in Greenland occurs *after* productivity increases at Lake Suigetsu – for example, during GI 12 and GI 2 (Fig. 4 and Fig. S7).

However, unlike the broadly coherent timing between Japanese and Chinese records with Lake Suigetsu over millennial-timescales, which fall within their respective age uncertainties, comparisons with the Greenland ice core record fall outside these uncertainty margins

(Fig. S7). Although Adolphi et al. (2018) reduced age uncertainties in the NGRIP record by aligning radiocarbon data with the Hulu Cave speleothem chronology (Fig. S7), the tuning is only applicable up to 45 cal ka BP. The potential lags in the Greenland record nonetheless warrant further investigation – particularly with North Atlantic climate archives with more precisely constrained chronologies – given the conservative, however increased age uncertainties associated with ice-layer counting in the Greenland cores. Regardless, Lake Suigetsu exhibits more gradual and symmetrical transitions between stadial and interstadial conditions, in contrast to the abrupt ‘saw-tooth’ characteristic of the Greenland interstadials. Despite millennial-scale cyclicity in both records, there are potential timing offsets and structural differences which may arise from comparing different proxies, chronological techniques, or fundamental differences in the climatic drivers.

While there are some similarities between the Lake Suigetsu and Greenland records, certain features of the Lake Suigetsu record appear to be correlated with Antarctic ice core $\delta^{18}\text{O}$ (Fig. 4). The EPICA Dronning Maud Land (EDML) $\delta^{18}\text{O}$ record shows periods of warming that align with strengthening of the EASM inferred from Lake Suigetsu during GI 12 and 2 – both of which occur prior to warming in Greenland. This pattern is consistent with some studies of Chinese speleothems that note correlations between monsoon intensity and Antarctic temperature, as well as a more Antarctic-like climate signature and a varying lead-lag relationship with Greenland (Barker and Knorr, 2007; Beck et al., 2018; Cai et al., 2006; Cheng et al., 2020; Liang et al., 2022; Rohling et al., 2009). Interpretations of these speleothem records, including those from Hulu and Xiaobailong Caves, suggest a combination of Northern and Southern Hemisphere climate influences on the Asian Monsoon, with the relative influence of each varying through time (Rohling et al., 2003, 2009). This dual-signal hypothesis is suggested to be driven by the temperature contrast between the hemispheres which influences monsoon intensity by modulating cross-equatorial airflow and movement of the ITCZ (An et al., 2000; Liang et al., 2022; Schneider et al., 2014).

While warm interstadial periods at Lake Suigetsu more closely resemble Antarctic ice core $\delta^{18}\text{O}$, cold stadials appear to correlate with Greenland ice core $\delta^{18}\text{O}$ (Fig. 4 and Fig. S7). Notably, prolonged Greenland stadials that coincide with significant freshwater discharges from the North American ice sheet into the North Atlantic – known as Heinrich events, or Heinrich Stadials (HS) – exhibit strong similarities to periods of low productivity at Lake Suigetsu. This is particularly evident during HS 5, 4, 3, and 2 (Fig. 4). These low productivity periods at Lake Suigetsu also align with periods of low speleothem $\delta^{18}\text{O}$ values in China and Japan, as well as lower TOC at Lakes Biwa and Nojiri (Mori et al., 2018). Lakes Biwa and Nojiri also show multiple episodes of low productivity – particularly during GI 12, 11, and 10 – that are not reflected in other records (Fig. 4 and Fig. S7). The coherence across records during HS periods highlights a possible link between prolonged North Atlantic cooling and weakening of the East Asian summer monsoon, resulting in cool and dry climate over East Asia. This weakening may be attributed to an enhanced southward migration of the ITCZ, which allows cold air from the North Atlantic to move over the dry Eurasian landmass via the westerlies and south of the Tibetan Plateau, as suggested for the last glacial-Holocene transition at Lake Suigetsu (Nakagawa et al., 2003, 2021). This airmass then delivers cold and dry conditions to China and Japan, overriding the influence of cross-equatorial airflow from the Southern Hemisphere on the monsoon.

While we observe both similarities and differences between productivity at Lake Suigetsu and ice core records from Greenland and Antarctica, further investigation of climate fluctuations recorded in precisely dated climate archives from the North Atlantic and Pacific is crucial for understanding the climate significance of the Lake Suigetsu record and its role in the context of global climate teleconnections. Furthermore, measuring additional palaeoclimate proxies, such as oxygen isotopes, in the Lake Suigetsu sediments would be highly valuable for validating the observations made from the bulk geochemical data.

6. Conclusion

Currently, there is no consensus about the spatial drivers that influenced the East Asian monsoon during the last glacial period, a time marked by abrupt climate change events. The limited availability of diverse, high-resolution, and continuously resolved environmental archives has compromised the understanding of the intricate processes affecting the intensity of the East Asian monsoon in the context of global climate change.

In this study, we used Fourier transform infrared spectroscopy (FTIR) on sediments from Lake Suigetsu, Japan, to develop a record of lake primary productivity and lake water mixing between 55 and 20 cal ka BP. We interpret these data to reflect changes in the intensity of the East Asian summer and winter monsoons. Our interpretations are validated by similarities on millennial timescales with other palaeoclimate records from Japan and China, including the Hulu Cave speleothems.

Our data supports an existing interpretation that millennial-scale intensity of the East Asian monsoon is influenced by a combination of process in both the Northern and Southern Hemispheres - further challenging the dominant view that the East Asian monsoon in Japan is primarily driven by the North Atlantic and westerly winds. This hypothesis suggests a greater, but dynamic, influence from Southern Hemisphere temperature on monsoon intensity which varies over time. Evidence for this is reflected in the timing and structure of interstadial transitions observed in both the Lake Suigetsu records and the Antarctic EDML ice core, particularly during Greenland Interstadials 12 and 2.

Conversely, during prolonged cold stadials associated with Heinrich events, there is coherence between weakening of the East Asian summer monsoon – as inferred from the Lake Suigetsu records and other archives from Japan and China – and the NGRIP Greenland ice core record. We propose that this North Atlantic connection emerges during extreme climate events in the North Atlantic that override other influences on the East Asian monsoon, including those originating from the Southern Hemisphere.

Further research is needed to explore this interpretation. Particularly, comparisons with North Atlantic and Pacific climate archives with more constrained age errors are crucial, given the uncertainties associated with layer counting in the Greenland and Antarctic ice cores. Future studies should aim to validate the Lake Suigetsu data presented here using additional proxies which mechanistically relate to temperature or hydroclimate variability. This will help compare abrupt climate events during the last glacial period and enhance our understanding of the complex drivers influencing the East Asian monsoon.

CRediT author statement

Vanessa Nowinski: Software, Validation, Formal analysis, Investigation, Data curation, Writing – Original Draft, Writing- Review & Editing, Visualisation. **Alexander Francke:** Conceptualisation, Methodology, Software, Validation, Investigation, Data curation, Writing-Review & Editing, Supervision. **John Tibby:** Investigation, Writing-Review & Editing, Supervision. **Takeshi Nakagawa:** Methodology, Software, Writing- Review & Editing. **Tony Hall:** Data curation, writing-Review & Editing. **Ikuko Kitaba:** Field work (coring). **Jonathan Tyler:** Conceptualisation, Methodology, Software, Investigation, Writing- Review & Editing, Supervision, Project administration, Funding acquisition.

Declaration of competing interest

The authors declare that they have no known competing financial interests or personal relationships that could have appeared to influence the work reported in this paper.

Acknowledgements

This project was supported by the ARC Discovery Project DP200101768. Vanessa Nowinski received funding through a University of Adelaide-funded PhD, and Jonathan Tyler was supported by ARC Future Fellowship FT230100648. Funding for core acquisition was led by Prof. Ryuji Tada. Drilling of the SG12 Lake Suigetsu sediment core was carried out by Seibushisui Co. Ltd. We thank Keitaro Yamada and Yoshiaki Suzuki for their contributions to the SG12 correlation model, and in particular, Yoshiaki Suzuki for their assistance during coring. We also gratefully acknowledge Jack Pedley, Lucy Stokes, and William Wyche for their laboratory assistance.

Appendix A. Supplementary data

Supplementary data to this article can be found online at <https://doi.org/10.1016/j.quascirev.2025.109624>.

Data availability

All data and/or code is contained within the submission.

References

- Adolphi, F., Bronk Ramsey, C., Erhardt, T., Edwards, R.L., Cheng, H., Turney, C.S., Cooper, A., Svensson, A., Rasmussen, S.O., Fischer, H., 2018. Connecting the Greenland ice-core and U/ Th timescales via cosmogenic radionuclides: testing the synchrony of dansgaard-Oeschger events. *Clim. Past* 14 (11), 1755–1781.
- Albert, P.G., McLean, D., Buckland, H.M., Suzuki, T., Jones, G., Staff, R.A., Vineberg, S., Kitaba, I., Yamada, K., Moriwaki, H., 2024. Cryptotephra preserved in Lake Suigetsu (SG14 core) reveals the eruption timing and distribution of ash fall from Japanese volcanoes during the late-glacial to early Holocene. *Quat. Sci. Rev.* 324, 108376.
- An, Z., Porter, S.C., Kutzbach, J.E., Wu, X., Wang, S., Liu, X., Li, X., Zhou, W., 2000. Asynchronous Holocene optimum of the East Asian monsoon. *Quat. Sci. Rev.* 19 (8), 743–762.
- Anderson, R.Y., Dean, W.E., 1988. Lacustrine varve formation through time. *Palaeogeography, Palaeoclimatology, Palaeoecology* 62 (1–4), 215–235.
- Bahrig, B., 1988. Palaeo-Environment Information from Deep Water Siderite (Lake of Laach, West Germany), 40. Geological Society Special Publication, pp. 153–158.
- Bahrig, B., 1989. Stable isotope composition of siderite as an indicator of the paleoenvironmental history of oil shale lakes. *Palaeogeogr. Palaeoclimatol. Palaeoecol.* 70 (1–3), 139–151.
- Barker, P., 1992. Differential diatom dissolution in late Quaternary sediments from Lake Manyara, Tanzania: an experimental approach. *J. Paleolimnol.* 7, 235–251.
- Barker, S., Knorr, G., 2007. Antarctic climate signature in the Greenland ice core record. *Proc. Natl. Acad. Sci. USA*. 104 (44), 17278–17282.
- Battarbee, R., Jones, V., Flower, R., Cameron, N., Bennion, H., Carvalho, L., Juggins, S., 2001. Diatoms. In: Smol, J., Birks, H., Last, W. (Eds.), *Environmental Change Using Lake Sediments* (Vol. 3 Terrestrial, Algal and Siliceous Indicator, pp. 155–202).
- Battarbee, R.W., Mackay, A., Jewson, D., Ryves, D., Sturm, M., 2005. Differential dissolution of Lake Baikal diatoms: correction factors and implications for palaeoclimatic reconstruction. *Global Planet. Change* 46 (1–4), 75–86.
- Beck, J.W., Zhou, W., Li, C., Wu, Z., White, L., Xian, F., Kong, X., An, Z., 2018. A 550,000-year record of East Asian monsoon rainfall from ^{10}Be in loess. *Science* 360 (6391), 877–881.
- Berner, R.A., 1971. *Principles of Chemical Sedimentology*, 240. McGraw-Hill, New York.
- Blunier, T., Chappelaz, J., Schwander, J., Dällenbach, A., Stauffer, B., Stocker, T., Raynaud, D., Jouzel, J., Clausen, H., Hammer, C., 1998. Asynchrony of Antarctic and Greenland climate change during the last glacial period. *Nature* 394 (6695), 739–743.
- Bouchet, M., Landais, A., Grisart, A., Parrenin, F., Prié, F., Jacob, R., Fourré, E., Capron, E., Raynaud, D., Lipenkov, V.Y., 2023. The Antarctic ice core chronology 2023 (AICC2023) chronological framework and associated timescale for the European Project for Ice Coring in Antarctica (EPICA) dome C ice core. *Clim. Past* 19 (11), 2257–2286.
- Bradbury, P., Cumming, B., Laird, K., 2002. A 1500-year record of climatic and environmental change in Elk Lake, Minnesota III: measures of past primary productivity. *J. Paleolimnol.* 27, 321–340.
- Broecker, W., 2010. *The Great Ocean Conveyor: Discovering the Trigger for Abrupt Climate Change*. Princeton University Press.
- Broecker, W.S., 1998. Paleocean circulation during the last deglaciation: a bipolar seesaw? *Paleoceanography* 13 (2), 119–121.
- Bronk Ramsey, C., Heaton, T.J., Scholz, G., Staff, R.A., Bryant, C.L., Brauer, A., Lamb, H.F., Marshall, M.H., Nakagawa, T., 2020. Reanalysis of the atmospheric radiocarbon calibration record from Lake Suigetsu, Japan. *Radiocarbon* 62 (4), 989–999.
- Bronk Ramsey, C., Staff, R.A., Bryant, C.L., Brock, F., Kitagawa, H., Van Der Plicht, J., Scholz, G., Marshall, M.H., Brauer, A., Lamb, H.F., 2012. A complete terrestrial radiocarbon record for 11.2 to 52.8 kyr BP. *Science* 338 (6105), 370–374.

- Buizert, C., Cuffey, K., Severinghaus, J., Baggenstos, D., Fudge, T., Steig, E., Markle, B., Winstrup, M., Rhodes, R.H., Brook, E.J., 2015. The WAIS Divide deep ice core WD2014 chronology—part 1: methane synchronization (68–31 ka BP) and the gas age–ice age difference. *Clim. Past* 11 (2), 153–173.
- Cai, Y., An, Z., Cheng, H., Edwards, R.L., Kelly, M.J., Liu, W., Wang, X., Shen, C.-C., 2006. High-resolution absolute-dated Indian Monsoon record between 53 and 36 ka from Xiaobailong Cave, southwestern China. *Geology* 34 (8), 621–624.
- Chen, W., Graf, H.-F., Huang, R., 2000. The interannual variability of East Asian Winter Monsoon and its relation to the summer monsoon. *Adv. Atmos. Sci.* 17 (1), 48–60.
- Chen, W., Wang, L., Feng, J., Wen, Z., Ma, T., Yang, X., Wang, C., 2019. Recent progress in studies of the variabilities and mechanisms of the East Asian monsoon in a changing climate. *Adv. Atmos. Sci.* 36, 887–901.
- Cheng, H., Edwards, R.L., Broecker, W.S., Denton, G.H., Kong, X., Wang, Y., Zhang, R., Wang, X., 2009. Ice age terminations. *Science* 326 (5950), 248–252.
- Cheng, H., Zhang, H., Spotl, C., Baker, J., Sinha, A., Li, H., Bartolomé, M., Moreno, A., Kathayat, G., Zhao, J., 2020. Timing and structure of the Younger Dryas event and its underlying climate dynamics. In: Proceedings of the National Academy of Sciences, 117, pp. 23408–23417, 38.
- Chiang, J.C.H., Fung, I.Y., Wu, C.-H., Cai, Y., Edman, J.P., Liu, Y., Day, J.A., Bhattacharya, T., Mondal, Y., Labrousse, C.A., 2015. Role of seasonal transitions and westerly jets in East Asian paleoclimate. *Quat. Sci. Rev.* 108, 111–129.
- Chukanov, N.V., 2013. Infrared Spectra of Mineral Species: Extended Library. Springer Science & Business Media.
- Cohen, A.S., 2003. Paleolimnology: the History and Evolution of Lake Systems. Oxford University Press.
- Colman, S.M., Peck, J., Karabanov, E., Carter, S.J., Bradbury, J., King, J., Williams, D., 1995. Continental climate response to orbital forcing from biogenic silica records in Lake Baikal. *Nature* 378 (6559), 769–771.
- Conley, D.J., Schelske, C.L., 2001. Biogenic silica. In: Tracking Environmental Change Using Lake Sediments: Terrestrial, Algal, and Siliceous Indicators, pp. 281–293.
- Corrick, E.C., Drysdale, R.N., Hellstrom, J.C., Capron, E., Rasmussen, S.O., Zhang, X., Fleitmann, D., Couchoud, I., Wolff, E., 2020. Synchronous timing of abrupt climate changes during the last glacial period. *Science* 369 (6506), 963–969.
- Curtis, C., Spears, D., 1968. The formation of sedimentary iron minerals. *Econ. Geol.* 63 (3), 257–270.
- Dansgaard, W., Clausen, H.B., Gundestrup, N., Hammer, C., Johnsen, S., Kristinsdottir, P., Reeh, N., 1982. A new Greenland deep ice core. *Science* 218 (4579), 1273–1277.
- Ditlevsen, P., Ditlevsen, S., 2023. Warning of a forthcoming collapse of the Atlantic meridional overturning circulation. *Nat. Commun.* 14 (1), 1–12.
- Douglas, M.S., Smol, J.P., 2010. Freshwater diatoms as indicators of environmental change in the High Arctic. In: The Diatoms: Applications for the Environmental and Earth Sciences, p. 249.
- Dykoski, C.A., Edwards, R.L., Cheng, H., Yuan, D., Cai, Y., Zhang, M., Lin, Y., Qing, J., An, Z., Revenaugh, J., 2005. A high-resolution, absolute-dated Holocene and deglacial Asian monsoon record from Donge Cave, China. *Earth Planet. Sci. Lett.* 233 (1–2), 71–86.
- Flower, R.J., 1993. Diatom preservation: experiments and observations on dissolution and breakage in modern and fossil material. In: Twelfth International Diatom Symposium: Proceedings of the Twelfth International Diatom Symposium, Renesse, the Netherlands, 30 August–5 September 1992.
- Fortin, M.-C., Gajewski, K., 2009. Assessing the use of sediment organic, carbonate and biogenic silica content as indicators of environmental conditions in Arctic lakes. *Polar Biol.* 32 (7), 985–998.
- Francke, A., Tyler, J.J., Staff, R., McLean, D., Nowinski, V., Saito-Kato, M., Tibby, J., Ikehara, M., Yokoyama, Y., Gotanda, K., 2025. Orbital-scale East Asian monsoon variability since the last interglacial inferred from the sediments of Lake Suigetsu, Japan. *Quat. Sci. Rev.* 368, 109566.
- Fukusawa, H., Kato, M., Fujiwara, O., 2002. Changes of eco-systems in the Last 500 Years Caused by Human Impacts in Lake Suigetsu, Central Japan, 37. Geographical Reports of Tokyo Metropolitan University, pp. 41–49.
- Gao, X., Shi, Y., Zhang, D., Wu, J., Giorgi, F., Ji, Z., Wang, Y., 2012. Uncertainties in monsoon precipitation projections over China: results from two high-resolution RCM simulations. *Clim. Res.* 52, 213–226.
- Geological Survey of Japan, 2002. NISHIZU. Geological map, 1:50,000. Geological survey by Nakae, S., Komatsubara, T., Naito, K. (1997–2000). Geological Survey of Japan.
- Giresse, P., Maley, J., Kelts, K., 1991. Sedimentation and palaeoenvironment in crater lake Barombi Mbo, Cameroon, during the last 25,000 years. *Sediment. Geol.* 71 (3), 151–175.
- He, C., 2023. Future drying subtropical East Asia in winter: mechanism and observational constraint. *J. Clim.* 36 (9), 2985–2998.
- Heinrich, H., 1988. Origin and consequences of cyclic ice rafting in the northeast Atlantic Ocean during the past 130,000 years. *Quat. Res.* 29 (2), 142–152.
- Huang, R., Chen, J., Wang, L., Lin, Z., 2012. Characteristics, processes, and causes of the spatio-temporal variabilities of the East Asian monsoon system. *Adv. Atmos. Sci.* 29, 910–942.
- Imboden, D.M., Wüest, A., 1995. Mixing mechanisms in lakes. In: Physics and Chemistry of Lakes. Springer, pp. 83–138.
- Iwamoto, N., Inouchi, Y., 2007. Reconstruction of millennial-scale variations in the East Asian summer monsoon over the past 300 ka based on the total carbon content of sediment from Lake Biwa, Japan. *Environ. Geol.* 52, 1607–1616.
- Japanese Meteorological Agency, 2025. Tsuruga (Fukui Prefecture) JMA Weather Station Data, Electronic Dataset, Japanese Meteorological Agency viewed 23/07/ 2025.
- Kamatani, A., 1982. Dissolution rates of silica from diatoms decomposing at various temperatures. *Mar. Biol.* 68, 91–96.
- Katsuta, N., Takano, M., Kawakami, S.-i., Togami, S., Fukusawa, H., Kumazawa, M., Yasuda, Y., 2007. Advanced micro-XRF method to separate sedimentary rhythms and event layers in sediments: its application to lacustrine sediment from Lake Suigetsu, Japan. *J. Paleolimnol.* 37 (2), 259–271.
- Kelly, M.J., Edwards, R.L., Cheng, H., Yuan, D., Cai, Y., Zhang, M., Lin, Y., An, Z., 2006. High resolution characterization of the Asian Monsoon between 146,000 and 99,000 years BP from Donge Cave, China and global correlation of events surrounding Termination II. *Palaeogeogr. Palaeoclimatol. Palaeoecol.* 236 (1–2), 20–38.
- Kelts, K., Hsü, K., 1978. Freshwater carbonate sedimentation. In: Lakes: Chemistry, Geology, Physics. Springer, pp. 295–323.
- Kigoshi, T., Kumon, F., Hayashi, R., Kuriyama, M., Yamada, K., Takemura, K., 2014. Climate changes for the past 52 ka clarified by total organic carbon concentrations and pollen composition in Lake Biwa, Japan. *Quat. Int.* 333, 2–12.
- Kossler, A., Tarasov, P., Schlolaut, G., Nakagawa, T., Marshall, M., Brauer, A., Staff, R., Ramsey, C.B., Bryant, C., Lamb, H., 2011. Onset and termination of the late-glacial climate reversal in the high-resolution diatom and sedimentary records from the annually laminated SG06 core from Lake Suigetsu, Japan. *Palaeogeogr. Palaeoclimatol. Palaeoecol.* 306 (3–4), 103–115.
- Kudo, Y., Kumon, F., 2012. Paleolithic cultures of MIS 3 to MIS 1 in relation to climate changes in the central Japanese islands. *Quat. Int.* 248, 22–31.
- Kumon, F., Kawai, S., Inouchi, Y., 2003. Climate changes between 25,000 and 6,000 yrs BP deduced from TOC, TN, and fossil pollen analyses of a sediment core from Lake Nojiri, central Japan. The Quaternary Research (daiyonki-kenkyū) 42 (1), 13–26.
- Lacey, J.H., Leng, M.J., Francke, A., Sloane, H.J., Milodowski, A., Vogel, H., Baumgarten, H., Zanchetta, G., Wagner, B., 2016. Northern Mediterranean climate since the middle Pleistocene: a 637 ka stable isotope record from Lake Ohrid (Albania/Macedonia). *Biogeosciences* 13 (6), 1801–1820.
- Lawrimore, J.H., Menne, M.J., Gleason, B.E., Williams, C.N., Wuertz, D.B., Vose, R.S., Rennie, J., 2011. An overview of the global Historical climatology network monthly mean temperature data set, version 3. *J. Geophys. Res. Atmos.* 116 (D19).
- Lehmann, M.F., Bernasconi, S.M., Barbieri, A., McKenzie, J.A., 2002. Preservation of organic matter and alteration of its carbon and nitrogen isotope composition during simulated and in situ early sedimentary diagenesis. *Geochem. Cosmochim. Acta* 66 (20), 3573–3584.
- Leng, M.J., Wagner, B., Boehm, A., Panagiotopoulos, K., Vane, C.H., Snelling, A., Haidon, C., Woodley, E., Vogel, H., Zanchetta, G., Banesci, I., 2013. Understanding past climatic and hydrological variability in the mediterranean from Lake Prespa sediment isotope and geochemical record over the last glacial cycle. *Quat. Sci. Rev.* 66, 123–136.
- Leuschner, D.C., Sirocko, F., 2000. The low-latitude monsoon climate during dansgaard–oeschger cycles and Heinrich events. *Quat. Sci. Rev.* 19 (1–5), 243–254.
- Lewin, J.C., 1961. The dissolution of silica from diatom walls. *Geochem. Cosmochim. Acta* 21 (3–4), 182–198.
- Li, Q., England, M.H., Hogg, A.M., Rintoul, S.R., Morrison, A.K., 2023. Abyssal ocean overturning slowdown and warming driven by Antarctic meltwater. *Nature* 615 (7954), 841–847.
- Liang, Y., Zhao, K., Wang, Y., Edwards, R.L., Cheng, H., Shao, Q., Chen, S., Wang, J., Zhu, J., 2022. Different response of stalagmite $\delta^{18}\text{O}$ and $\delta^{13}\text{C}$ to millennial-scale events during the last glacial, evidenced from Huangjin Cave, northhrn China. *Quat. Sci. Rev.* 276, 107305.
- Liang, Y.J., Wang, Y.J., Wang, Q., Wu, J.Y., Shao, Q.F., Zhang, Z.Q., Yang, S.H., Kong, X. G., Edwards, R.L., 2019. East Asian summer monsoon climates and cave hydrological cycles over dansgaard–oeschger events 14 to 11 revealed by a new stalagmite record from hulu Cave. *Quat. Res.* 92 (3), 725–737.
- Lu, H., Wang, X., Wang, Y., Zhang, X., Yi, S., Wang, X., Stevens, T., Kurbanov, R., Marković, S.B., 2022. Chinese loess and the Asian monsoon: what we know and what remains unknown. *Quat. Int.* 620, 85–97.
- Marshall, M., Schlolaut, G., Nakagawa, T., Lamb, H., Brauer, A., Staff, R., Ramsey, C.B., Tarasov, P., Gotanda, K., Haraguchi, T., 2012. A novel approach to varve counting using μXRF and X-radiography in combination with thin-section microscopy, applied to the late glacial chronology from Lake suigetsu, Japan. *Quat. Geochronol.* 13, 70–80.
- Masuzawa, T., Kitano, Y., 1982. Sulfate reduction and sulfur fixation in sediment of a historically meromictic lake, Lake Suigetsu, Japan. *J. Oceanogr. Soc. Jpn.* 38, 21–27.
- McKay, N.P., Kaufman, D.S., Michelutti, N., 2008. Biogenic silica concentration as a high-resolution, quantitative temperature proxy at Hallet Lake, south-central Alaska. *Geophys. Res. Lett.* 35 (5).
- McLean, D., Albert, P.G., Nakagawa, T., Suzuki, T., Staff, R.A., Yamada, K., Kitaba, I., Haraguchi, T., Kitagawa, J., Members, S.P., 2018. Integrating the Holocene tephrostratigraphy for East Asia using a high-resolution cryptotephra study from Lake suigetsu (SG14 core), central Japan. *Quat. Sci. Rev.* 183, 36–58.
- McMinn, A., 1995. Comparison of diatom preservation between oxic and anoxic basins in Ellis Fjord, Antarctica. *Diatom Res.* 10 (1), 145–151.
- Menviel, L., Timmermann, A., Friedrich, T., England, M.H., 2014. Hindcasting the continuum of dansgaard–oeschger variability: mechanisms, patterns and timing. *Clim. Past* 10 (1), 63–77.
- Meyers, P.A., Ishiwatari, R., 1993. Lacustrine organic geochemistry—an overview of indicators of organic matter sources and diagenesis in lake sediments. *Org. Geochem.* 20 (7), 867–900.
- Meyers, P.A., Takemura, K., Horie, S., 1993. Reinterpretation of late Quaternary sediment chronology of Lake Biwa, Japan, from correlation with marine glacial-interglacial cycles. *Quat. Res.* 39 (2), 154–162.
- Mingram, J., Stebich, M., Schettler, G., Hu, Y., Rioual, P., Nowaczyk, N., Dulski, P., You, H., Opitz, S., Liu, Q., 2018. Millennial-scale East Asian monsoon variability of the last glacial deduced from annually laminated sediments from Lake Sihaiblongwan, NE China. *Quat. Sci. Rev.* 201, 57–76.

- Mori, T., Kashiwagi, K., Amekawa, S., Kato, H., Okumura, T., Takashima, C., Wu, C.-C., Shen, C.-C., Quade, J., Kano, A., 2018. Temperature and seawater isotopic controls on two stalagmite records since 83 ka from maritime Japan. *Quat. Sci. Rev.* 192, 47–58.
- Nagashima, K., Tada, R., Tani, A., Sun, Y., Isozaki, Y., Toyoda, S., Hasegawa, H., 2011. Millennial-scale oscillations of the westerly jet path during the last glacial period. *J. Asian Earth Sci.* 40 (6), 1214–1220.
- Nakagawa, T., Gotanda, K., Haraguchi, T., Danhara, T., Yonenobu, H., Brauer, A., Yokoyama, Y., Tada, R., Takemura, K., Staff, R.A., Payne, R., Ramsey, C.B., Bryant, C., Brock, F., Scholz, G., Marshall, M., Tarasov, P., Lamb, H., Suigetsu, P., 2012. SG06, a fully continuous and varved sediment core from Lake Suigetsu, Japan: stratigraphy and potential for improving the radiocarbon calibration model and understanding of late Quaternary climate changes. *Quat. Sci. Rev.* 36, 164–176.
- Nakagawa, T., Kitagawa, H., Yasuda, Y., Tarasov, P.E., Nishida, K., Gotanda, K., Sawai, Y., Y. R. C. P. M., 2003. Asynchronous climate changes in the North Atlantic and Japan during the last termination. *Science* 299 (5607), 688–691.
- Nakagawa, T., Tarasov, P., Staff, R., Ramsey, C.B., Marshall, M., Scholz, G., Bryant, C., Brauer, A., Lamb, H., Haraguchi, T., Gotanda, K., Kitaba, I., Kitagawa, H., van der Plicht, J., Yonenobu, H., Omori, T., Yokoyama, Y., Tada, R., Yasuda, Y., Suigetsu Project, M., 2021. The spatio-temporal structure of the Lateglacial to early Holocene transition reconstructed from the pollen record of Lake Suigetsu and its precise correlation with other key global archives: implications for palaeoclimatology and archaeology. *Global Planet. Change* 202.
- Naughten, K.A., Holland, P.R., De Rydt, J., 2023. Unavoidable future increase in West Antarctic ice-shelf melting over the twenty-first century. *Nat. Clim. Change* 13 (11), 1222–1228.
- Oeschger, H., Beer, J., Siegenthaler, U., Stauffer, B., Dansgaard, W., Langway, C., 1984. Late glacial climate history from ice cores. *Climate Processes and Climate Sensitivity* 29, 299–306.
- Ozawa, A., Ueda, A., Fantong, W.Y., Anazawa, K., Yoshida, Y., Kusakabe, M., Ohba, T., Tanyileke, G., Hell, J.V., 2017. Rate of siderite precipitation in Lake Nyos, Cameroon. *Geol. Soc. Spec. Publ.* 437 (1), 213–222.
- Pearson, E.J., Juggins, S., Tyler, J., 2014. Ultrahigh resolution total organic carbon analysis using Fourier transform near infrared reflectance spectroscopy (FT-NIRS). *G-cubed* 15 (1), 292–301.
- Petit, J.-R., Jouzel, J., Raynaud, D., Barkov, N.I., Barnola, J.-M., Basile, I., Bender, M., Chappellaz, J., Davis, M., Delaygue, G., 1999. Climate and atmospheric history of the past 420,000 years from the Vostok ice core, Antarctica. *Nature* 399 (6735), 429–436.
- Porter, S.C., An, Z., 1995. Correlation between climate events in the North Atlantic and China during the last glaciation. *Nature* 375 (6529), 305–308.
- Prokopenko, A.A., Karababan, E.B., Williams, D.F., Kuzmin, M.I., Shackleton, N.J., Crowhurst, S.J., Peck, J.A., Gvozdov, A.N., King, J.W., 2001. Biogenic silica record of the Lake Baikal response to climatic forcing during the Brunhes. *Quat. Res.* 55 (2), 123–132.
- Rasmussen, S.O., Bigler, M., Blockley, S.P., Blunier, T., Buchardt, S.L., Clausen, H.B., Cvijanovic, I., Dahl-Jensen, D., Johnsen, S.J., Fischer, H., 2014. A stratigraphic framework for abrupt climatic changes during the last Glacial period based on three synchronized Greenland ice-core records: refining and extending the INTIMATE event stratigraphy. *Quat. Sci. Rev.* 106, 14–28.
- Reimer, P.J., Austin, W.E., Bard, E., Bayliss, A., Blackwell, P.G., Ramsey, C.B., Butzin, M., Cheng, H., Edwards, R.L., Friedrich, M., 2020. The IntCal20 Northern Hemisphere radiocarbon age calibration curve (0–55 cal kBP). *Radiocarbon* 62 (4), 725–757.
- Reimer, P.J., Bard, E., Bayliss, A., Beck, J.W., Blackwell, P.G., Ramsey, C.B., Buck, C.E., Cheng, H., Edwards, R.L., Friedrich, M., 2013. IntCal13 and Marine13 radiocarbon age calibration curves 0–50,000 years cal BP. *Radiocarbon* 55 (4), 1869–1887.
- Rex, C.L., Staff, R.A., Sanderson, D.C.W., Cresswell, A.J., Marshall, M.H., Hyodo, M., Horiuchi, D., Tada, R., Nakagawa, T., 2022. Controls on luminescence signals in lake sediment cores: a study from Lake Suigetsu, Japan. *Quat. Geochronol.* 71, 101319.
- Rex, C.L., Tyler, J.J., Nagaya, K., Staff, R.A., Leng, M.J., Yamada, K., Kitaba, I., Kitagawa, J., Kojima, H., Nakagawa, T., 2024. The contemporary stable isotope hydrology of Lake Suigetsu and surrounding catchment (Japan) and its implications for sediment-derived palaeoclimate records. *Quaternary Science Advances* 13, 100145.
- Rohling, E., Mayewski, P., Challenor, P., 2003. On the timing and mechanism of millennial-scale climate variability during the last glacial cycle. *Clim. Dyn.* 20, 257–267.
- Rohling, E.J., Liu, Q.S., Roberts, A.P., Stanford, J.D., Rasmussen, S.O., Langen, P.L., Siddall, M., 2009. Controls on the East Asian monsoon during the last glacial cycle, based on comparison between Hulu Cave and polar ice-core records. *Quat. Sci. Rev.* 28 (27), 3291–3302.
- Rosén, P., Vogel, H., Cunningham, L., Hahn, A., Hausmann, S., Pienitz, R., Zolitschka, B., Wagner, B., Persson, P., 2011. Universally applicable model for the quantitative determination of lake sediment composition using Fourier transform infrared spectroscopy. *Environ. Sci. Technol.* 45 (20), 8858–8865.
- Rosén, P., Vogel, H., Cunningham, L., Reuss, N., Conley, D.J., Persson, P., 2010. Fourier transform infrared spectroscopy, a new method for rapid determination of total organic and inorganic carbon and biogenic silica concentration in lake sediments. *J. Paleolimnol.* 43, 247–259.
- Ryves, D.B., Juggins, S., Fritz, S.C., Battarbee, R.W., 2001. Experimental diatom dissolution and the quantification of microfossil preservation in sediments. *Palaeogeogr. Palaeoclimatol. Palaeoecol.* 172 (1–2), 99–113.
- Saito-Kato, M., Yamada, K., Staff, R.A., Nakagawa, T., Yonenobu, H., Haraguchi, T., Takemura, K., Bronk Ramsey, C., 2013. An assessment of the magnitude of the AD 1586 Tensho tsunami inferred from Lake Suigetsu sediment cores. *J. Geogr.* 122 (3), 493–501.
- Sawada, K., Arita, Y., Nakamura, T., Akiyama, M., Kamei, T., Nakai, N., 1992. 14C Dating of the Nojiri-ko Formation Using Accelerator Mass Spectrometry.
- Schelske, C.L., Conley, D.J., Stoermer, E.F., Newberry, T.L., Campbell, C., 1987. Biogenic silica and phosphorus accumulation in sediments as indices of eutrophication in the Laurentian Great Lakes. In: *Paleolimnology IV: Proceedings of the Fourth International Symposium on Paleolimnology*, Held at Ossiach, Carinthia, Austria.
- Schiemann, R., Lüthi, D., Schär, C., 2009. Seasonality and interannual variability of the westerly jet in the Tibetan Plateau region. *J. Clim.* 22 (11), 2940–2957.
- Scholz, G., Marshall, M.H., Brauer, A., Nakagawa, T., Lamb, H.F., Staff, R.A., Ramsey, C.B., Bryant, C.L., Brock, F., Kossler, A., 2012. An automated method for varve interpolation and its application to the late glacial chronology from Lake Suigetsu, Japan. *Quat. Geochronol.* 13, 52–69.
- Scholz, G., Staff, R.A., Brauer, A., Lamb, H.F., Marshall, M.H., Ramsey, C.B., Nakagawa, T., 2018. An extended and revised Lake Suigetsu varve chronology from ~ 50 to 10 ka BP based on detailed sediment micro-facies analyses. *Quat. Sci. Rev.* 200, 351–366.
- Schneider, T., Bischoff, T., Haug, G.H., 2014. Migrations and dynamics of the intertropical convergence zone. *Nature* 513 (7516), 45–53.
- Schulz, H., Von Rad, U., Erlenkeuser, H., 1998. Correlation between Arabian Sea and Greenland climate oscillations of the past 110,000 years. *Nature* 393 (6680), 54–57.
- Seierstad, I.K., Abbott, P.M., Bigler, M., Blunier, T., Bourne, A.J., Brook, E., Buchardt, S.L., Buiertz, C., Clausen, H.B., Cook, E., 2014. Consistently dated records from the Greenland GRIP, GISP2 and NGRIP ice cores for the past 104 ka reveal regional millennial-scale δ18O gradients with possible Heinrich event imprint. *Quat. Sci. Rev.* 106, 29–46.
- Shen, C.-C., Kano, A., Hori, M., Lin, K., Chiu, T.-C., Burr, G.S., 2010. East Asian monsoon evolution and reconciliation of climate records from Japan and Greenland during the last deglaciation. *Quat. Sci. Rev.* 29 (23–24), 3327–3335.
- Smith, V.C., Staff, R.A., Blockley, S.P., Ramsey, C.B., Nakagawa, T., Mark, D.F., Takemura, K., Danhara, T., 2013. Identification and correlation of visible tephra in the Lake Suigetsu SG06 sedimentary archive, Japan: chronostratigraphic markers for synchronising of east Asian/west Pacific palaeoclimatic records across the last 150 ka. *Quat. Sci. Rev.* 67, 121–137.
- Sobek, S., Durisch-Kaiser, E., Zurbriggen, R., Wongfun, N., Wessels, M., Pasche, N., Wehrli, B., 2009. Organic carbon burial efficiency in lake sediments controlled by oxygen exposure time and sediment source. *Limnol. Oceanogr.* 54 (6), 2243–2254.
- Staff, R.A., Sanderson, D.C.W., Rex, C.L., Cresswell, A., Hyodo, M., Kitaba, I., Marshall, M.H., Scholz, G., Yamada, K., Suzuki, Y., Nowinski, V., Tada, R., Nakagawa, T., 2024. A luminescence-derived cryptostratigraphy from the Lake Suigetsu sedimentary profile, Japan: 45,000–30,200 IntCal20 yr BP. *Quat. Geochronol.* 83, 101588.
- Staff, R.A., Scholz, G., Ramsey, C.B., Brock, F., Bryant, C.L., Kitagawa, H., Van der Plicht, J., Marshall, M.H., Brauer, A., Lamb, H.F., 2013. Integration of the old and new Lake Suigetsu (Japan) terrestrial radiocarbon calibration data sets. *Radiocarbon* 55 (4), 2049–2058.
- Stumm, W., Morgan, J.J., 2012. *Aquatic Chemistry: Chemical Equilibria and Rates in Natural Waters*. John Wiley & Sons.
- Suzuki, Y., Tada, R., Nagashima, K., Nakagawa, T., Gotanda, K., Haraguchi, T., Scholz, G., 2021. Extreme flood events and their frequency variations during the middle to late-Holocene recorded in the sediment of Lake Suigetsu, central Japan. *Holocene* 31 (1), 121–133.
- Swann, G.E., Patwardhan, S., 2011. Application of Fourier transform infrared spectroscopy (FTIR) for assessing biogenic silica sample purity in geochemical analyses and palaeoenvironmental research. *Clim. Past* 7 (1), 65–74.
- Tada, R., Irino, T., Koizumi, I., 1999. Land-ocean linkages over orbital and millennial timescales recorded in late Quaternary sediments of the Japan Sea. *Paleoceanography* 14 (2), 236–247.
- Tyler, J., Kashiyama, Y., Ohkouchi, N., Ogawa, N., Yokoyama, Y., Chikaraishi, Y., Staff, R., Ikebara, M., Bronk Ramsey, C., Bryant, C., 2010. Tracking aquatic change using chlorin-specific carbon and nitrogen isotopes: the last glacial-interglacial transition at Lake Suigetsu, Japan. *G-cubed* 11 (9).
- Vuillemin, A., Mayr, C., Schuessler, J.A., Friese, A., Bauer, K.W., Lücke, A., Heuer, V.B., Glombitza, C., Henny, C., von Blanckenburg, F., 2023. A one-million-year isotope record from siderites formed in modern ferruginous sediments. *GeoSci. World. Bulletin*, 135 (1–2), 504–522.
- Vuillemin, A., Wirth, R., Kemnitzi, H., Schleicher, A.M., Friese, A., Bauer, K.W., Simister, R., Nomotsu, S., Ordoñez, L., Ariztegui, D., 2019. Formation of diagenetic siderite in modern ferruginous sediments. *Geology* 47 (6), 540–544.
- Wang, B., Wu, R., Fu, X., 2000. Pacific–East Asian teleconnection: how does ENSO affect East Asian climate? *J. Clim.* 13 (9), 1517–1536.
- Wang, Y., Cheng, H., Edwards, R.L., Kong, X., Shao, X., Chen, S., Wu, J., Jiang, X., Wang, X., An, Z., 2008. Millennial-and orbital-scale changes in the East Asian monsoon over the past 224,000 years. *Nature* 451 (7182), 1090–1093.
- Wang, Y.J., Cheng, H., Edwards, R.L., An, Z.S., Wu, J.Y., Shen, C.C., Dorale, J.A., 2001. A high-resolution absolute-dated late pleistocene monsoon record from Hulu Cave, China. *Science* 294 (5550), 2345–2348.
- White, W.B., 1974. The carbonate minerals. In: Farmer, V.C. (Ed.), *The Infrared Spectra of Minerals*, 4. Mineralogical Society of Great Britain and Ireland.
- Xiao, J., Inouchi, Y., Kumai, H., Yoshikawa, S., Kondo, Y., Liu, T., An, Z., 1997. Biogenic silica record in Lake Biwa of central Japan over the past 145,000 years. *Quat. Res.* 47 (3), 277–283.
- Xu, Z., Fan, K., 2022. Inter-model spreading of changes in East Asian winter monsoon circulation under 1.5 and 2.0° C global warming targets. *Int. J. Climatol.* 42 (8), 4360–4378.

- Ye, X., Anderson, E.J., Chu, P.Y., Huang, C., Xue, P., 2019. Impact of water mixing and ice formation on the warming of Lake Superior: a model-guided mechanism study. *Limnol. Oceanogr.* 64 (2), 558–574.
- You, Q., Jiang, Z., Yue, X., Guo, W., Liu, Y., Cao, J., Li, W., Wu, F., Cai, Z., Zhu, H., Li, T., Liu, Z., He, J., Chen, D., Pepin, N., Zhai, P., 2022. Recent frontiers of climate changes in East Asia at global warming of 1.5°C and 2°C. *npj Climate. Atmo. Sci.* 5 (1), 80.
- Yuan, D., Cheng, H., Edwards, R.L., Dykoski, C.A., Kelly, M.J., Zhang, M., Qing, J., Lin, Y., Wang, Y., Wu, J., 2004. Timing, duration, and transitions of the last interglacial Asian monsoon. *Science* 304 (5670), 575–578.